

# Influence of the particle size of electrode materials on intercalation rate and capacity of new electrodes

R. Vacassy<sup>a,\*</sup>, H. Hofmann<sup>a</sup>, N. Papageorgiou<sup>b</sup>, M. Grätzel<sup>b</sup>

<sup>a</sup> Powder Technology Laboratory (LTP), Department of Materials Science, Swiss Federal Institute of Technology (EPFL), CH-1015 Lausanne, Switzerland

<sup>b</sup> Laboratory of Photonics and Interfaces (LPI / ICP2), Department of Chemistry, Swiss Federal Institute of Technology (EPFL), CH-1015 Lausanne, Switzerland

## Abstract

A mesoscopic form of the spinel  $\text{LiMn}_2\text{O}_4$  has been synthesized and studied for its electrochemical performance as a lithium ion insertion host material and for its application in the electrode fabrication destined for rechargeable batteries. A theoretical model based on the sintering behavior of several commercial materials indicated the major importance of controlling the particle size and the morphology of the agglomerates with respect to power density and fast lithium intercalation in a prospective thin-layer battery system. Computational models were developed for complete mesoporous thin-layer cell simulation at steady state, providing insight to the requirements concerning the electrolyte function in the 'rocking-chair' concept scale-up. A complete thin-layer battery was conceived and constructed which showed promising performance. © 1999 Elsevier Science S.A. All rights reserved.

**Keywords:** Cathode material;  $\text{LiMn}_2\text{O}_4$ ; Particle size; Electrochemical characterization

## 1. Introduction

$\text{LiMn}_2\text{O}_4$  has shown a great potential for application as the positive electrode for Li Batteries. The preparation of inorganic colloids, such as  $\text{LiMn}_2\text{O}_4$ , can be achieved by various solution reactions such as the sol-gel method [1] and the hydrolysis reaction [2]. The size, the shape, the morphology of the particles and its chemical composition determine strongly the physical and chemical properties of solid  $\text{LiMn}_2\text{O}_4$ , which need to be well defined for applications as positive intercalation electrode [3]. Of particular significance are problems related to the dependence of the particle/agglomerate morphology and structure on the electrochemical performances of the material [4]. In order to improve power density and lithium intercalation kinetics in a prospective thin-layer battery system, the 'neural network' theory has been applied to the positive electrode material [5]. Based on the sintering properties of commercial powders, the improvement of the particle size distribution of  $\text{LiMn}_2\text{O}_4$  powders should conduct to a better green density and, as a result, to an improved interconnectivity [6].

Three basic directions of exploratory research have been pursued in order to investigate the feasibility of the

above three fundamental premises for accumulator development exploiting lithium ion technology and particularly the 'rocking-chair' concept. First, the investigation of the influence of particle size on cathode micro-kinetics with regards to the reversible  $\text{Li}^+$  intercalation reaction in spinel  $\text{LiMn}_2\text{O}_4$ . Second, the search for, as well as the examination of the application feasibility, of novel solvent or molten salt/electrolyte systems either synthesized by our group or commercially available, in terms of electrochemical/chemical stability and their suitability as lithium ion cell components. Third, the mass-transfer modeling of the thin-layer nanocrystalline electrode able to provide insight into the requirements of an effective electrolyte under any given steady-state performance conditions and physical cell/electrode configuration, which in combination with the previous two investigations, would ultimately indicate the scale-up potential of this system. This has embodied the safety aspect by considering only non-water sensitive and low toxicity materials for electrodes and electrolytes.

## 2. Experimental

$\text{LiMn}_2\text{O}_4$  powders were synthesized in aqueous solution by reacting different manganate salts with LiOH under

\* Corresponding author

basic pH conditions. Four manganate salt precursors were selected, in order to investigate the effect of counter-ion (e.g., the anion) on the precipitation reactions: manganate acetate, manganate acetylacetonate (Acac), manganate fluoride and manganate orthophosphate.

The precipitation of  $\text{LiMn}_2\text{O}_4$  precursor particles was performed starting from homogeneous solutions of manganate salt at 0.13 M and  $\text{LiOH}$  at 1.3 M with a  $[\text{Li}]/[\text{Mn}^{3+}]$  ratio equals to 10 for each precipitation reaction. The reaction temperature was fixed at  $110^\circ\text{C}$  and the pH of the reactants was increased to basic values ( $\sim 12$ – $13$ ) using the concentrated  $\text{LiOH}$  solution. In each experiment, the manganate salt solution and the  $\text{LiOH}$  solution were separately dissolved, before mixing them in a batch reactor with agitation. The solution was dark and it was really difficult to appreciate visually the beginning of the precipitation. The reaction time was fixed at 2 h after which the hydrolytic reaction between  $\text{LiOH}$  and the manganate salt was terminated by rapidly cooling the solution to less than  $10^\circ\text{C}$  in an ice bath. As-precipitated  $\text{LiMn}_2\text{O}_4$  powders were then centrifuged at 4000 rpm, washed twice with water to eliminate unreacted products and three times with isopropanol. The cleaned powders were dried overnight at  $50^\circ\text{C}$  until complete evaporation of the solvent, and then calcined at  $600^\circ\text{C}$  (1 h, slow heating rate).

Agglomerated micrometer and submicrometer particles were formed under these conditions. Depending on the associated anion, variations in particle size were observed, as it was also observed for the  $\text{ZnS}$  synthesis in a recent work [7]. Characteristics of synthesized powders are given in Table 1.  $\text{LiMn}_2\text{O}_4$  powders were characterized by nitrogen adsorption at 77 K (BET, Micromeritics) and X-ray diffractometry using  $\text{CuK}_\alpha$  radiation (Inel CPS-120). After preparation, the particle structure, morphology and sizes were investigated by scanning electron microscopy (SEM, Philips XL 30).

Thin film electrodes were prepared by casting aqueous mixtures of prepared manganate powders with PVA (MW 100 000) as binder and graphite particles (Lonza KS-10 or carbon nanotubes) as the conducting matrix. The weight percentage of the constituents was chosen 3% PVA and 10% graphite. In one situation, carbon nanotubes were added to the paste blends. The pastes were cast on conductive tin oxide (CTO) substrates at ambient temperature, dried and then heated in an air furnace for 15 min at

$200^\circ\text{C}$ . As electrolyte, a 1 M  $\text{LiClO}_4$  in propylene carbonate was the standard in all electrode cycling experiments to enable objective comparison. Cyclic voltammetry was used to elucidate the kinetic aspects of the lithium insertion/extraction in the oxides of the above thin film electrodes. Electrochemical characterizations of as-prepared powders were conducted on  $\text{LiMn}_2\text{O}_4$  pellets which contained 50% graphite (XC72) and 2% Teflon. A ball mixing was carried out during 10 min for a better homogeneity of the powder mixture.

### 3. The neural network approach

More than 30 alumina powders were characterized regarding the green density of the compacted part, a particle packing characteristic also called envelop density, versus some powder properties (particle size distribution, specific surface area and particle shape) [6]. A detailed description of the neural network theory can be found elsewhere [5]. Such results were extrapolated to the case of  $\text{LiMn}_2\text{O}_4$  by taking into account the physical properties of such cathode material. Assuming a Li diffusion coefficient in  $\text{LiMn}_2\text{O}_4$  of  $5 \times 10^{-10} \text{ cm}^2/\text{s}$ , the Li diffusion in the host material, and as a result, the charge density, could be estimated as a function of particle diameters and/or specific surface. The calculations show that an optimal particle size with respect to the charge density is found to be within  $0.5$ – $0.8 \mu\text{m}$  ( $\sim 1.7$ – $2.9 \text{ m}^2/\text{g}$ ).

For faster charge and discharge of the battery, the interfaces between oxide and electrolyte should be as larger as possible. Nanoparticles with a large specific surface area of about  $50 \text{ m}^2/\text{cm}^3$  (particle size of 60 to 80 nm), such as  $\text{LiMn}_2\text{O}_4$  powders from acetate or Acac, are well-adapted for this requirement. In Fig. 1, the specific surface area was calculated for powders with a broad agglomerate size distribution. The maximum specific charge density is found to be  $0.34 \text{ Ah}/\text{cm}^3$  with a  $8 \text{ m}^2/\text{cm}^3$  surface area. This result shows clearly that with both optimized powder synthesis and optimized powder processing, even higher specific charge densities with high specific surface area can be obtained (Fig. 1, arrow direction). However, the optimization of powder synthesis can only be done by an experimental approach. A slight sintering of the primary particles in order to obtain a better

Table 1  
Characteristics of synthesized  $\text{LiMn}_2\text{O}_4$  powders

	Ligands			
	Acetate	Acac	Fluoride	Orthophosphate
Particle morphology	Nearly spherical	Nearly spherical	Hard spherical aggregate	Cubical + spherical
$S_{\text{BET}}$ ( $\text{m}^2/\text{g}$ )	24	25	5	4
Crystalline phase	Spinel	Spinel	Spinel	Spinel
SEM/TEM particle diameter (nm)	50	50	bimodal (50 + 1000) + large agglomerates	300–400 + large agglomerates

The sample names refer to the specific ligand involved in the synthesis.

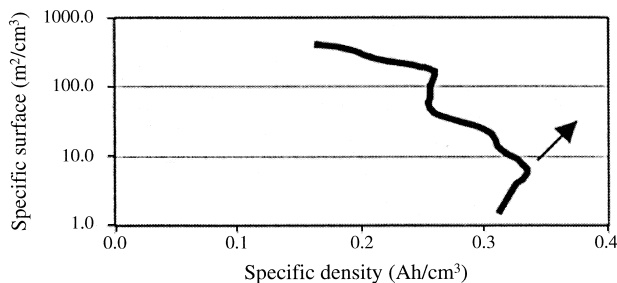


Fig. 1. Specific surface as a function of charge density for powder compacts. The specific capacity of the positive electrode has to be increased in the arrow direction.

interconnectivity should therefore be determinant to performance.

## 4. Results

### 4.1. Scope and option evaluation

The spinel  $\text{LiMn}_2\text{O}_4$  has been studied as the cathode material for rechargeable lithium batteries because it is less expensive, less toxic, and can be prepared by an easier method than, e.g., the cobalt oxides. However, the performance of lithium ion rechargeable cells is mostly limited by the diffusion of the lithium ion into the host material. Further improvements of the charge–discharge performance of  $\text{LiMn}_2\text{O}_4$  composite electrodes can be expected by designing an electrode structure of the host oxide with a nanoscale character. The morphology should play a fundamental role in the electrode properties [8]. It has been demonstrated that the capacities of  $\text{LiMn}_2\text{O}_4$  electrodes could be enhanced by decreasing the average grain size of the oxide [9].

The kinetics of reversible lithium insertion should also be enhanced by reduction of the particle size of the oxide. In the charge–discharge reaction, diffusion of  $\text{Li}^+$  in the  $\text{LiMn}_2\text{O}_4$  often determines the overall rate because its diffusion coefficient is as small as  $5 \times 10^{-10} \text{ cm}^2/\text{s}$ , and the diffusion in the oxide becomes too slow to follow the applied reaction rate. The thickness of the oxide layer across which a lithium ion must travel can be reduced considerably by reducing the size of the primary grain size. The shorter diffusion length makes the mean kinetics faster, resulting in a better utilization of  $\text{LiMn}_2\text{O}_4$ , especially at higher current density. However, an improved interconnectivity can only be reached making use of  $\text{LiMn}_2\text{O}_4$  powders of large particle/agglomerate size distribution with a median diameter of about  $0.7 \mu\text{m}$ , as predicted by the ‘neural network’ theory. Therefore, controlling the particle size distribution of the electrode material, with an addition of a given amount of nanostructured material, should largely define the application limits of a performing cell. Moreover, the 4-V  $\text{Li}^+$  extraction-interca-

lation regime was chosen for this study, as the intended matching of the cathode material with any other anode would provide the highest possible energy and power density for the prospective battery system.

On the other hand, the  $\text{Li}^+$  contained and transferred via the electrolyte should be effectively supplied to and removed from every point within the solid electrode during insertion and extraction, respectively. In order to rationalize the action of the electrolyte phase the mass-transfer of a thin layer cell at steady-state operation (constant current delivered) has been modeled, providing a first approach perception of the possible limitations imposed by the electrolyte function for given physical cell geometry, diffusion/electrolyte parameters and current passed during charging or delivered during discharging.

### 4.2. Thin layer electrode preparation, characterization and kinetic performance

Some preliminary experiments were carried out to estimate the kinetic performances of the cathode material as a function of particle size. Electrodes from micrometer-sized, commercial powders display higher irreversibility than the electrode from the mesoporous nanopowder ( $\text{LiMn}_2\text{O}_4$  from Acac) sintered at  $700^\circ\text{C}$ . Moreover, the addition of graphite in the mesoporous material results in electrodes of very low capacity and low reversibility, while addition of nanotubes improves markedly both capacity and reversibility. Nevertheless, the best performances were obtained using a thin sintered layer of  $\text{LiMn}_2\text{O}_4$  nanoparticles. The sintered nanoparticulate layer was 1.5 mm thick and showed a very porous structure ( $\sim 70\%$ , as estimated by mass to surface measurements). The behaviour of such cathode material was studied by cyclic voltammetry as it is seen in Fig. 2.

A close to theoretical capacity (148 mAh/g or 532 Cb/g) is derived for these electrodes when considering a layer of 70% porosity. The two insertion levels for the spinel in the 4 Volts range reported in the literature for 200 nm layers at  $0.05 \text{ mV/s}$ , appear very distinct for our 1.5 mm thickness recorded at a sweep rate over two orders of magnitude higher [10]. This demonstrates the high reversibility attainable by decreasing the particle size to the nanometer range and simultaneously ensuring effective particle connectivity.

### 4.3. Electrochemical performance of $\text{LiMn}_2\text{O}_4$ powders

Electrochemical characterizations (Fig. 3) were carried out on both the as-prepared nanopowder (from Acac) and on a mixture of nanometer- and submicrometer-sized particles ( $d_{50} = 0.8 \mu\text{m}$ , large size distribution). It is clearly shown that the specific charge of the powder mixture is better compared to that of the nanoparticulate powder. This result confirms the assumption from the ‘neural network’

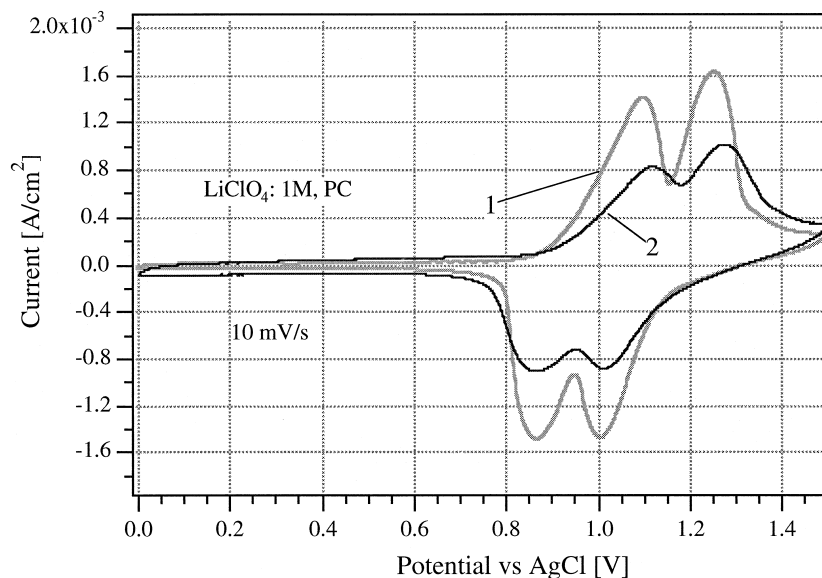


Fig. 2. Cyclic voltammetry of sintered nanostructured  $\text{LiMn}_2\text{O}_4$  (prepared from Acac) layers. (1)  $1.5 \mu\text{m}$  layer calcined at  $700^\circ\text{C}$ , the reversible integrated charge is  $46 \text{ mCb}/\text{cm}^2$ , (2)  $1.5 \mu\text{m}$  layer calcined at  $400^\circ\text{C}$  and integrated charge  $36 \text{ mCb}/\text{cm}^2$ .

theory which indicated that the electrochemical performances of powders with large particle size distribution would be improved as compared with nanoparticle of narrower size distribution. Because of a better green density of the powder mixture, the particle interconnectivity inside the positive electrode is enhanced. After 5 cycles, a higher irreversible capacity (4%), an indicative result, is obtained with the powder mixture which needs to be minimized to ensure a better cycleability of the cathode material. On the other hand, the nanoparticulate material seems to be more stable to cycle because of a lower irreversible capacity (2–3%). However, variations of spe-

cific charge of these two powders could also be interpreted in terms of crystallinity of spinel material. These two approaches show that the synthesis and processing of the  $\text{LiMn}_2\text{O}_4$  materials have further to be optimized in terms of particle size distribution and crystallographic composition.

#### 4.4. Thin layer cell mass-transport model

We have developed a diffusion–migration model of a thin-layer cell comprising mesoporous electrodes. The cell configuration consists of two 1 mm lithium intercalation

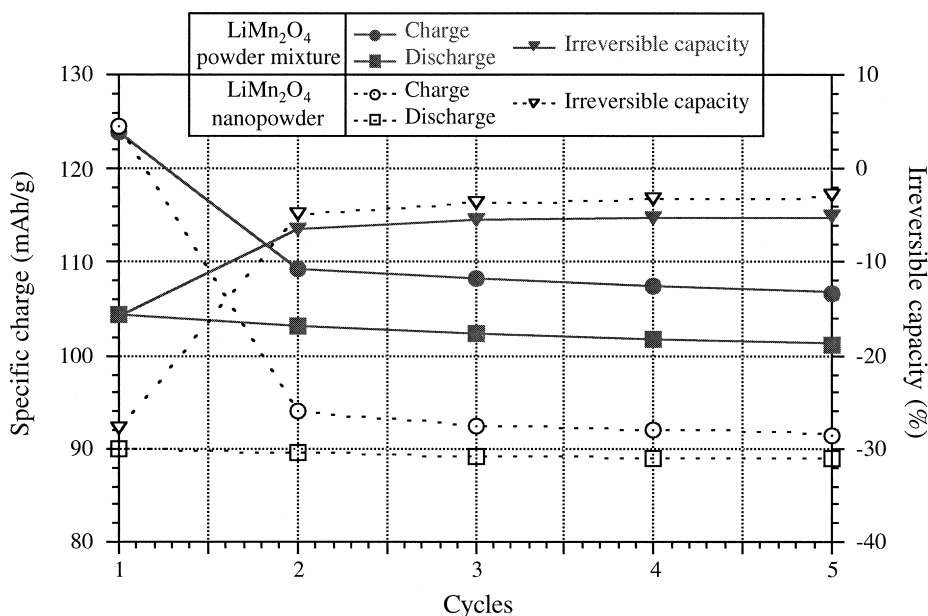


Fig. 3. Electrochemical characterization of two  $\text{LiMn}_2\text{O}_4$  powders.

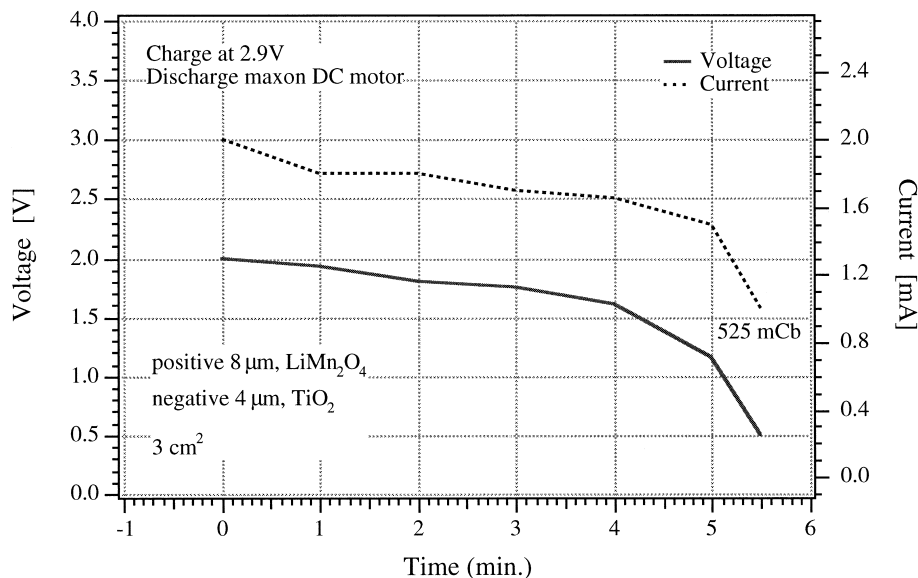


Fig. 4. Electrical performance of the thin-layer microbattery during the fifth discharge.

mesoporous hosts separated by a 20  $\mu\text{m}$  inert and insulating porous spacer. The initial electrolyte concentration in monovalent Li salt is 1 M and the free stream diffusion coefficient for  $\text{Li}^+$  in the electrolyte corresponds to the case of propylene carbonate ( $3 \times 10^{-6} \text{ cm}^2/\text{s}$ ) of approximately 3 cP. The electrode porosities were 50% and 90% for the spacer layer. Of course, anything smaller than 1000  $\mu\text{m}$  would increase the limiting currents. It is noted that the absence of supporting electrolyte in this case aids the lithium ion diffusion or transport but at a cost of potential in the form of IR drop across the cell. This calculation reveals that for electrodes of 10  $\mu\text{m}$  in the above configuration, currents as high as 500  $\text{mA}/\text{cm}^2$  are possible as far as electrolyte performance is concerned.

#### 4.5. Transfer to practice

A thin layer microbattery was conceived using the sintered  $\text{LiMn}_2\text{O}_4$  powder mixture as the cathode material, a mesoporous  $\text{TiO}_2$  negative electrode [11], and electrolytes containing the Li-imide salt with MPN or imidazolium molten salt. These electrolytes have the potential of delivering high discharge currents (above 1  $\text{mA}/\text{cm}^2$ ) in a voltage domain of 0.5–1.5 V vs. AgCl. A complete cell has been constructed with electrochemical characteristics presented in Fig. 4 (fifth discharge showed). This type of performance is promising and actually appears to exceed the requirements for lithium microgenerators suitable for commercialization.

## 5. Conclusion

This work has demonstrated the feasibility of a thin-layer microbattery constructed from a  $\text{LiMn}_2\text{O}_4$  powder mixture

as the cathode. The performance of the positive cathode could be improved making use of some powder technology aspects. The knowledge from the materials science might be helpful in the future to develop higher performance materials suitable for applications as electrode for Li insertion battery systems.

The development of mesoporous lithium manganate electrodes demands further research effort. In particular, active film/layer conductivity has to be improved by polymer/carbon matrix incorporation and optimization of particle size distribution and content of additives. The development of a comprehensive modeling of both the electrolyte and the solid diffusion phenomena in mesoporous layer or other configuration electrodes is necessary to further develop thicker electrode layer with good performance. To evaluate safety problems, some microcalorimetry measurements under operation conditions in order to ascertain the stability of electrodes, and possibly of complete cells, are underway.

## Acknowledgements

This work was supported by the Swiss Federal Office of Energy, Bern which is greatly acknowledged. The authors thank Dr. R. Imhof and Dr. P. Novák at Paul Scherrer Institute, Villigen for the electrochemical characterizations of the  $\text{LiMn}_2\text{O}_4$  powders and for fruitful discussions.

## References

- [1] P. Barboux, J.M. Tarascon, F.K. Shokoohi, J. Solid State Chem. 94 (1) (1991) 185.
- [2] C. Barriga, A. Calero, J. Morales, J.L. Tirado, React. Solids 7 (1989) 263.

- [3] M. Winter, J.O. Besenhard, M.E. Spahr, P. Novák, *Advanced Materials* 10 (10) (1998) 725.
- [4] G.S. Nagarajan, J.W. Van Zee, R.M. Spotnitz, *J. Electrochem. Soc.* 145 (3) (1998) 771.
- [5] G. Kateman, J.R.M. Smith, *Anal. Chim. Acta* 179 (1983) 277.
- [6] H. Hofmann, *Sintering Technology*, in: M. Dekker (Ed.), 1996, p. 301.
- [7] R. Vacassy, S.M. Scholz, J. Dutta, C.J.G. Plummer, R. Houriet, H. Hofmann, *J. Am. Ceram. Soc.* 81 (10) (1998) 2699.
- [8] S.D. Han, N. Treuil, G. Campet, J. Portier, C. Delmas, J.C. Lassegues, A. Pierre, *Mater. Sci. Forum* 152–155 (1994) 217.
- [9] F.K. Shokoohi, J.M. Tarascon, B.J. Wilkens, D. Guyomard, C.C. Chang, *J. Electrochem. Soc.* 139 (7) (1992) 1845.
- [10] W. Liu, G.C. Farrington, F. Chaput, B. Dunn, *J. Electrochem. Soc.* 143 (3) (1996) 879.
- [11] N. Papageorgiou, C. Barbé, M. Grätzel, *J. Phys. Chem. B* 102 (21) (1998) 4156.